Control of the Walker breakdown by periodical magnetic wire width modulation

Olga Lozhkina, Robert M. Reeve∗, Robert Frömter, and Mathias Kläui
Institute of Physics, Johannes Gutenberg University,
Mainz, 55128, Germany

Suppression of the Walker breakdown in confined wires is key to improving the operation and reliability of magnetic domain-wall-based devices including logic, memory, and sensor applications. Here, via micromagnetic simulations we demonstrate that a periodical wire width modulation with suitable geometric parameters can fully suppress the Walker breakdown of a field-driven domain wall, conserving its spin structure in the whole operating field range of a device. Key differences in the efficacy of the wire width modulation are observed for wires with different widths and thicknesses such that different domain wall states are energetically stable. In particular, the approach is found to be effective in expanding the field-operating window of a device in the case of smaller wire widths and thicknesses (below 150 nm wide and 15 nm thick), whereas in larger wires the advantages from the suppression in Walker breakdown are counteracted by the increase in domain wall pinning and the reduction in the nucleation field for new domain walls. Simulations on intersecting magnetic wires prove the importance of suppression of the Walker breakdown. Since the domain wall behaviour is chirality dependent, introducing periodical wire width modulation conserves the spin structure thus reducing stochasticity of the domain wall propagation.

I. INTRODUCTION

Domain walls (DWs) confined in magnetic wires [1] can be manipulated by applied magnetic fields or electrical currents, which together with various methods for the detection of magnetic domain orientation makes them of great interest for applications such as non-volatile logic [2], memory devices [3], and magnetic sensors [4-6]. Magnetic DW propagation in nanowires recently drew scientific attention as a medium for neuromorphic computing [7-9] due to its inherently stochastic behavior.

An important characteristic of a field-driven magnetic DW-based device is its field-operating window (FOW), which describes the field range where the device operates reliably. Often the FOW is described as an interval between DW depinning and nucleation regimes [10]. Below the depinning field the DW does not move under applied fields, whereas above the nucleation field new DWs are spontaneously created. Since both scenarios lead to device failure it is important to understand these regimes and for maximum flexibility and efficiency it is desirable to enlarge the FOW [11]. One particularly crucial problem for DW applications related to the lower end of the FOW is the high stochasticity of the DW pinning/depinning behavior [12–14]. In particular, many DW-based device concepts include complex geometrical features including curved wires [2,10], various notches [15] and intersection regions [11] where reliable DW propagation is challenging. Furthermore, real systems have material and processing related imperfections, and all these can serve as pinning centers, limiting the FOW and device reliability. DW propagation through such pinning centers is in particular strongly affected by the DW spin structure. Additionally, the DW propagation and spin structure has a complex dependence on the strength of the applied field [16,17]. At low fields, a steady motion is observed, where the DW propagation velocity depends linearly on the applied field [18]. Above a certain field threshold, called the Walker field, the DW velocity drops abruptly, a phenomenon known as Walker breakdown [18]. An associated periodical change of the DW spin configuration from a so-called transverse wall to a vortex wall and back, with a periodical rotation of the magnetization vector in the plane perpendicular to the magnetic wire, causes an oscillatory displacement of the DW over a distance known as the Walker period. Periodic DW spin-structure transformations above the Walker breakdown are caused by the finite value of the damping constant and the resulting interplay between the magnetostatic and the exchange energy. This regime is undesirable for the device operation due to the changing DW spin structure and low DW propagation velocities [19]. At even higher fields the DW exhibits again faster, but turbulent motion and more complex spin states with multiple vortices. Hence, the fast and steady propagation below the Walker breakdown is most robust and preferred for device applications. The Walker field depends crucially on the wire composition [20–22] and geometry [23], however in many studies the Walker field is lower than the field required to depin walls in the device. A thorough control over an external field projection driving the DW in a real device is often not possible. As a result, the devices need to operate above the Walker field within the highly stochastic oscillatory and turbulent DW propagation regimes. Therefore, for more reliable device operation it is necessary to understand how to either decrease the depinning field, or increase the Walker field, or both, in order to enable fast device operation within the steady propagation regime for the FOW.

In order to overcome some of these issues, various special approaches to the design of a magnetic wire have been considered and shown to drastically affect the DW motion, thus providing a route to achieving deterministic and

reliable DW propagation. First, the application of an oscillating longitudinal external magnetic field was found to suppress the Walker breakdown [24], however this is very hard to implement technically for devices. Alternatively, simulations of magnetic wires with random natural-like rough edges showed the suppression of the vortex nucleation associated with Walker breakdown and the transverse domain wall stabilization, which enables high domain wall velocities [25], although DW propagation in magnetic stripes undergoes the Walker breakdown at low fields in experiments [16]. On this basis, the periodic modulation of the magnetic wire width using different geometries (comb-like [26], introducing gaps [27], triangular features [28] or wavy wires [23,29–33]) was suggested as a way to generate a periodical stray field modulation and thus provide a controllable means to overcome the Walker breakdown. The viability of these approaches has been investigated in simulations [29-33] and experiments [22,30] on simple short straight wires. In particular, authors have proposed a wire-width modulation with a period smaller than the Walker period in order to disturb every spin structure transformation and thus to suppress the Walker breakdown [30]; simulations have demonstrated Walker breakdown suppression by introducing a 50 nm period modulation with fields up to 30 mT [29]. Enhanced robustness of the DW propagation through a magnetic wires' intersection with introducing wire width modulation and was observed in Ref. [32]. However, while the proof of concept of the physics of the wire width modulation has been shown, existing data on the wire width modulation is fragmentary and scattered. Furthermore, the details of the Walker breakdown suppression and in particular the optimal geometries for maximizing the field operating window and achieving efficient device operation necessary to employ the approach in both straight wires and more complex device elements such as intersections remain unknown, calling for further work.Considering all previously suggested modulation shapes this work focuses on sinusoidal modulation since this avoids sharp cusps and notches that could act as pinning or nucleation sites and is easier to realize on a small scale by means of electron beam lithography. Despite recent device concepts based on DW motion often using electrical current drive [13, 34-35], the study of domain wall propagation under external magnetic fields is still reasonable, since the basic patterns of the Walker breakdown suppression through disturbing vortex core formation in external field can be extended to the case of current drive. Besides, at present the only commercial application of domain wall propagation in a magnetic wire is a multiturn rotation sensor[4-5,36] that is controlled by an external magnetic field. It has room for improvement[6,11,33], in particular increasing the maximum number of turns counted. Engineering solutions are limited by the stochastic behaviour of the DWs and a way to displace DWs in magnetic wires in a controlled manner would spur the development of more DW applications.

In this paper we performed an extensive set of micromagnetic simulations of the DW propagation in soft magnetic wires across a large geometrical parameter space in order to gain a comprehensive understanding of the effectiveness of geometrical wire width modulation in suppressing the Walker breakdown. Our work links the periodical magnetic wire width modulation to the domain wall phase diagram, thereby explaining the variety of published results. The existence of multiple possible spin configurations of DWs in magnetic wires was demonstrated to be the main reason of the propagation stochasticity. Despite higher DW propagation velocities being attractive for applications, uncontrollable changes in the DW spin structure during propagation affect the device operation reliability. To this end, our investigation, unlike previous studies, is focused on the domain wall spin structure rather than its propagation velocity. Simulations were performed for various wire thicknesses (5-30 nm), widths (100-200 nm), modulation periods (45-1000 nm) and amplitudes (0-12%) in order to clarify the Walker breakdown suppression mechanism and to figure out conditions for optimal performance of future applications, including in complex device elements such as wire intersections which are vital components of various new concepts. The results are discussed in relation to the different DW spin structures and considering the FOW of the device.

II. METHODS

Micromagnetic simulations were performed with the MuMax3 [37] program at zero K temperature. Standard values for Py of $A_{ex} = 13 \cdot 10^{-12}$ J/m and $\alpha = 0.01$ [38] have been used for the exchange stiffness and the Gilbert damping. For the saturation magnetization $M_s = 7.95 \cdot 10^5$ A/m was used, as determined by means of superconducting quantum interference device (SQUID) for permalloy films grown in our lab. For static simulations, i.e. depinning and nucleation field detection, a larger value of $\alpha = 3$ [39] was used to speed up the relaxation. The cell size in the in-plane directions is 5 nm, which was chosen not to exceed the permalloy exchange length of $\Lambda = 5.7$ nm, and the full film thickness t in the out-of-plane direction. The geometries studied are permalloy wires with wavy edges following sinusoidal curves of fixed phase and opposite sign (Figure 1 inset). The thickness t remains constant, while the width is modulated between $w \pm 2a$, where w is the average width, a is the amplitude, and $t << w$. The simulated wire length is 6 μm mimicking an infinitely long wire. Before propagating the domain walls in the simulations, the wires were initialized with a DW positioned 500 nm away

from the end of the wire. The domain wall type was chosen based on the known DW phase diagram, taking into account the wire dimensions, and then the state was relaxed before applying the field along the wire to displace the wall. To find the nucleation fields additional simulations were performed with a ring in the vortex state with diameter d = 8 μm, $d >> w$. Applying an external in-plane field above the critical value (nucleation field) we observe the magnetisation switching with the formation of two DWs in the ring.

III. RESULTS

In order to understand the influence of periodic wire width modulation on domain wall propagation, we first perform micromagnetic simulations on field-induced domain wall propagation for different amplitudes of the modulation, while keeping the other geometrical parameters fixed. First we look at the simulated displacement of the DW vs. time in order to understand the propagation regimes [18]: at low applied fields the DW displacement changes linearly with time (Figure 1a, blue curve), then with increasing field above Walker breakdown one observes periodical reverse DW motion reflected in the oscillations in the graph and a dramatic drop of the DW velocity as seen by the change in the slope (Figure 1a, red curve), where the DW displacement over one time period is called the Walker period. Finally, at higher applied fields both the Walker and time periods gradually decrease, and the propagation becomes linear again (Figure 1a, green curve). The wire modulated at an amplitude of 3 % of its width in the right panel of Figure 1a demonstrates the same DW propagation mechanism as the unmodulated wire, but shifted towards higher magnetic fields. In order to visualize this, we extract the DW displacement vs. time slope to give the DW velocity as plotted in Figure 1b, along with the Walker period, as a function of the applied field.

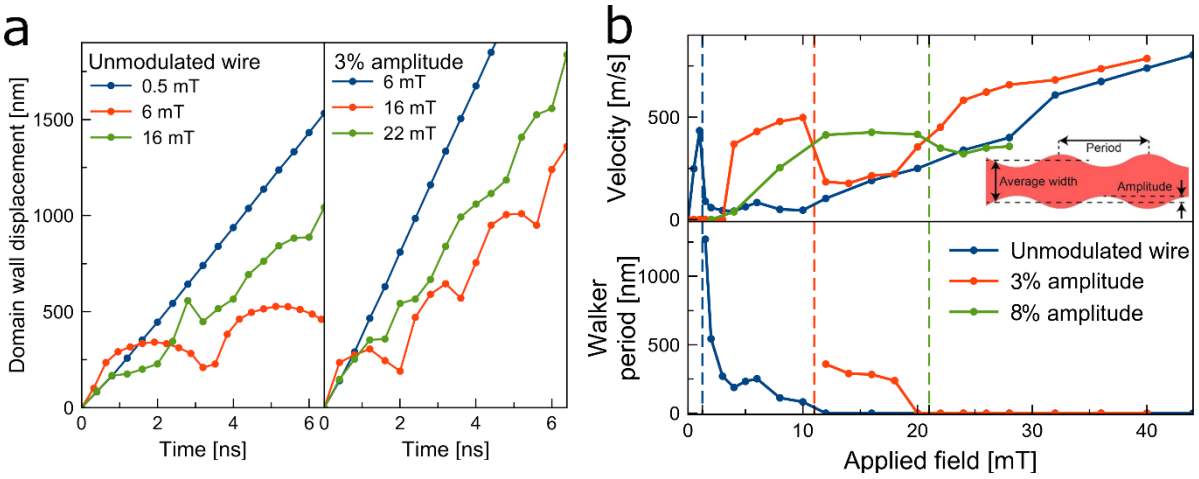

Figure. 1. (a) Domain wall displacement under external field as a function of time for an unmodulated and a modulated (50 nm period and 3% amplitude) magnetic wire with 12 nm thickness, 150 nm average width. Presented curves depict three DW propagation regimes: steady (blue), oscillatory (red) and turbulent (green). (b) Examples of DW velocities and Walker periods vs. applied field for magnetic wires with 12 nm thickness, 150 nm average width, 50 nm modulation period and 0, 3, and 8% modulation amplitudes (blue, red, and green curves respectively). The dotted vertical lines represent the Walker breakdown values for the corresponding wires. A schematic representation of the magnetic wire width modulation is shown in the inset.

The figure demonstrates exemplarily the way periodical wire width modulation affects the DW propagation. The graphs depict the simulated DW velocities and Walker periods for three magnetic wires with 150 nm average width, 12 nm thickness, 50 nm modulation period and 0, 3, and 8% modulation amplitude (blue, red, and green curves respectively). A schematic of the geometry can be seen in the inset. Corresponding snapshots from the simulations at certain time steps for selected field strengths of 6 and 16 mT are shown in Figure 2.

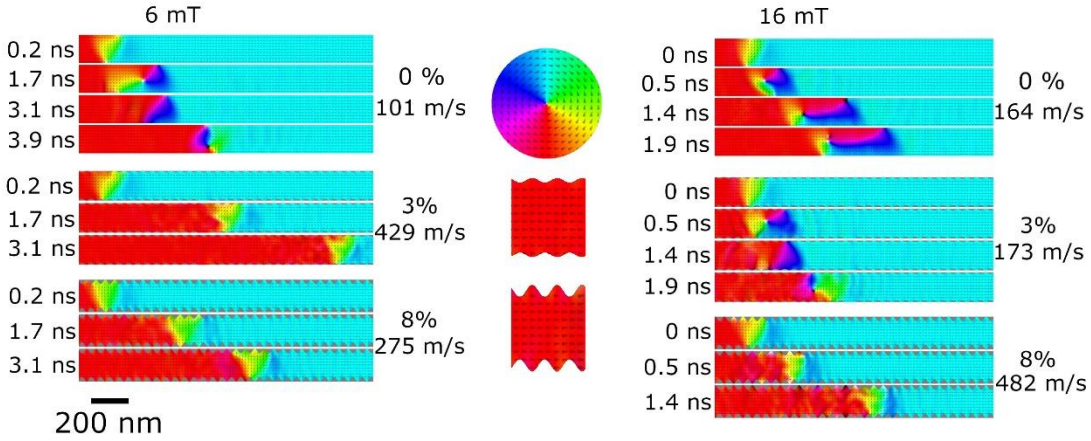

Figure. 2. Snapshots of sections of the micromagnetic simulations, demonstrating DW propagation through an unmodulated (0%) magnetic wire and wires with 3% and 8% modulation at certain time steps for selected field strengths of 6 mT (left) and 16 mT (right). The unmodulated wire demonstrates the DW spin-structure transformation, while transverse DWs propagate through the modulated wires unchanged at 6 mT. At 16 mT the 3% modulated wire also exhibits Walker breakdown accompanied by the DW structure transitions and a significant drop of the average DW velocity, as indicated on the right. In the center, a color wheel encoding the magnetization directions is given, together with enlarged sections of the modulated wires visalizing the used width modulation

For the unmodulated wire, as seen in the blue curve, one can see a linear velocity vs. field dependence below 2 mT, followed by an abrupt velocity drop corresponding to the onset of oscillating DW motion with a slow average velocity and periodic spin structure changes leading to a finite Walker period (depicted in Figure 2, 0% wire at 6 mT). Starting from 10 mT the DW propagation becomes turbulent (0% wire in Figure 2 at 16 mT) and the DW velocity rises approximately linearly again with increasing applied field. Only above 20 mT does the velocity approach and then exceed the velocities in the steady-motion regime. In this turbulent regime there is no well-defined change in spin structure and therefore the Walker period tends to zero.

The red curve demonstrates the case for 3% wire amplitude modulation. Here, there is no DW propagation below 4 mT, since the DW is pinned. With further increased applied field the DW is depinned and propagates steadily with increasing velocity up to the Walker breakdown at around 10 mT (the 3% wire in Figure 2 at 6 mT demonstrates such steady DW propagation and at 16 mT oscillatory motion). Above 18 mT turbulent motion is seen. Periodical magnetic wire width modulation shifts both the Walker breakdown and the transition between oscillatory and turbulent regimes towards higher fields and the oscillatory regime range shrinks significantly. The DW propagation in the turbulent regime demonstrates the same mechanism and similar velocities for both, modulated and unmodulated wires, as seen in Fig. 1b.

According to the Stoner-Wohlfarth model, the DW nucleation fields depend on the magnetic wire dimensions [10] as $H_n = \frac{1}{2} M_s \frac{t}{t+w}$ where t and w are the wire thickness and width respectively and M_s is the saturation magnetization. Due to the local wire widening, new undesired DWs are nucleated in the modulated wire at lower fields compared to the unmodulated wire (40 mT instead of 44 mT). Thus overall, the periodical wire width modulation with 3% amplitude expands the upper limit of the steady DW flow range from 2 mT to 6 mT, with a slight reduction of the oscillating DW propagation range, but also decreases the FOW (the range between the DW depinning and nucleation fields) from 44 mT for the unmodulated wire to 36 mT for 3% amplitude modulation. Furthermore, there is a small increase in the maximum steady state DW velocity. The green curves correspond to the larger modulation amplitude (8%). In this case the DW depinning field is pushed to even higher fields (5 mT) and the nucleation of new DWs occurs at lower fields (28 mT) which means the FOW shrinks to 23 mT from 44 mT in the case of the unmodulated wire. The DW propagation in the modulated wire demonstrates only steady motion at lower fields (8% wire in Figure 2) which becomes turbulent [10] above 21 mT. No oscillatory spin structure changes are seen and thus there is no defined Walker period. The DW velocity vs. applied field curves demonstrate a smaller slope for higher modulation amplitudes in the steady regime; this DW slowdown is another undesired effect of the wire width modulation on the DW propagation.

Having seen that the width modulation can increase the Walker field we would like to identify wire-width-modulation parameters that keep the Walker breakdown field above the new DW nucleation fields, such that DWs undergo steady motion throughout the FOW and the Walker breakdown is fully suppressed. A set of modulated wires with different thicknesses varied from 5 to 30 nm was simulated to ascertain the changes in DW propagation behaviour with varying initial DW states for a fixed width and modulation period (150 nm average width and 50

nm period). Transverse and vortex DWs can be stable or metastable depending on the magnetic wire width and thickness [15,40]; larger width and thickness wires tend to support vortex domain walls or more complex multi-DW states [39,41], while transverse DWs are stable for smaller widths and thicknesses. One might expect qualitatively different DW behaviour in these geometries. The simulated DW velocities as a function of both the applied field and the wire thickness are shown in a colour map in Figure 3 for the case of (a) 8% modulation and (b) no modulation. The boundaries of the DW depinning, new domain wall nucleation and for the onset of the Walker breakdown are indicated by the lines on the graph. Field values below which depinning, where no DW propagation is observed, and above nucleation, where new undesirable DWs arise in the wire, are marked dark blue and dark red, respectively. The unmodulated wire demonstrates no pinning in our simulations and the Walker fields do not exceed 1 mT for all geometries and thus are not presented in the graph. In the case of modulated wires the Walker fields can be outside the FOW (lower than the depinning field or higher than the nucleation field) which makes their determination impossible.

One can observe a fast Walker field decay with increasing wire thickness and a corresponding reduction of the width modulation efficiency for the modulated wire in Figure 3a, while no change in the propagation mechanism is observed in Figure 3b depicting the case of unmodulated wires. This highlights a qualitative difference in the effect of width modulation on DW propagation for wires with different widths and thicknesses.

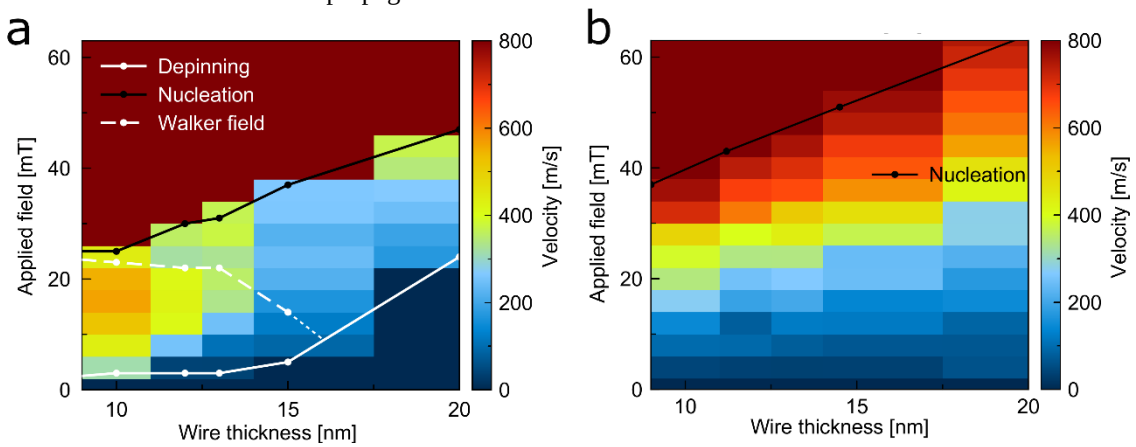

Figure 3. DW velocity colour maps vs. applied field and DW nucleation, depinning and Walker fields plotted vs. width modulation amplitude at fixed period (50 nm) and fixed amplitude (8%), for (a) width-modulated and (b) unmodulated magnetic wires, the average wire width is 150 nm. Black lines depict the nucleation field for new DWs, solid white lines represent the depinning field and dashed white lines represent the Walker field. The unmodulated wire demonstrates no pinning in our simulations and the Walker fields do not exceed 1 mT for all geometries and thus are not presented in the graph.

As mentioned before, according to the DW phase diagram [41] there are distinct ranges of permalloy wire widths and thicknesses providing stable transverse DWs (in the case of smaller widths and thicknesses) or vortex DWs (for larger widths and thicknesses). In order to separately investigate these two regimes, we simulated one set corresponding to energetically favourable transverse DWs (10 nm thickness, 100 nm width, 45-1000 nm modulation periods and 0-12% amplitudes) and a second set of simulations for stable vortex DWs (30 nm thickness, 200 nm width, 80-1000 nm modulation periods and 0-15% amplitudes).

Figure 4 depicts the DW velocity colour maps in a magnetic wire with a thickness and width that yields stable transverse DWs as the lowest energy static configuration (10 nm thick and 100 nm average width). Introducing a wire width modulation with increasing amplitude (Figure 4a) gradually increases the depinning field and decreases the nucleation field of DWs, which leads to the decrease of the FOW of devices based on DW propagation. Nevertheless, the modulation also gradually suppresses the Walker breakdown (gradual rise of the Walker field) which leads to an increase of the DW velocities. In the region of high-amplitude wire-width modulation (10-12% on the graph) the Walker field is pushed beyond the nucleation field and thus the DW propagation is steady in the whole FOW with velocities higher than for an unmodulated wire (amplitude 0% on the graph). Therefore, the Walker breakdown has been completely suppressed within the FOW. Figure 4b demonstrates the DW velocities for different modulation periods at a fixed width modulation amplitude of 10%. For large modulation periods we find a reduction of DW nucleation fields that can be attributed to the introduction of narrow areas of extended lengths in the magnetic wires, while the other DW behaviour characteristics remain similar to the unmodulated wire (low depinning and Walker fields, similar values of DW velocities). For small modulation periods a strong non-linearity in the dependence of the nucleation, depinning, and Walker fields on the modulation period is observed. The FOW is strongly reduced, but the Walker field remains above the nucleation field, indicating the

conservation of the DW spin structure within the FOW. For very small modulation periods of 45-50 nm we find very low DW depinning fields that are beneficial for applications.

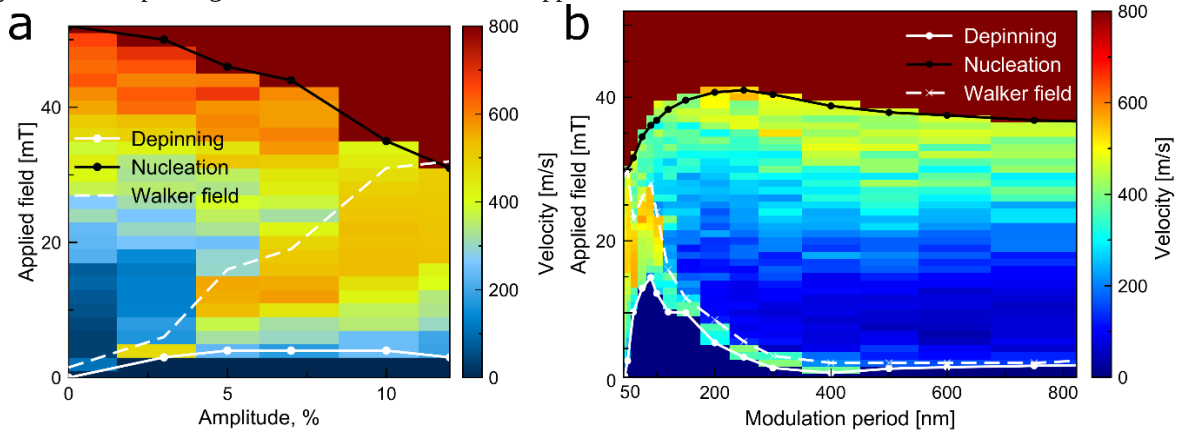

Figure 4. DW velocity colour maps vs. applied field and DW nucleation, depinning and Walker fields plotted vs. (a) width modulation amplitude at fixed period (50 nm) and (b) width modulation period at fixed amplitude (10%). The wire thickness is 10 nm and the average width is 100 nm. The initial domain wall configuration is a transverse DW, which remains stable below the Walker field.

Figure 5 in contrast demonstrates the DW propagation in thicker magnetic wires with larger widths. Here a very different behaviour is clearly seen: no significant gain in the Walker field is observed because of the much larger depinning fields, which are higher than or only just below the Walker field for the vortex walls. The nucleation fields exhibit a similar dependence on the wire width modulation amplitude to the case of the smaller widths and thicknesses, and the effect of the DW slowdown introduced by the wire width modulation appears in lower velocities in the region of higher modulation amplitudes in Figure 5a and in the region of smaller modulation period in Figure 5b.

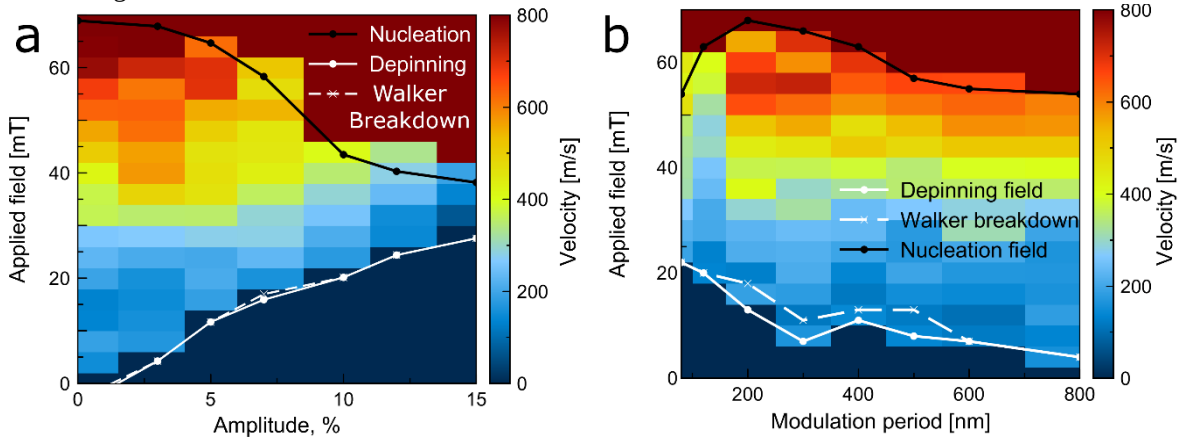

Figure 5. DW velocity colour maps vs. applied field and DW nucleation, depinning and Walker fields plotted vs. (a) width modulation amplitude at fixed period (80 nm) and (b) width modulation period at fixed amplitude (8%). The wire thickness is 30 nm and the average width is 200 nm. The initial domain wall configuration is a vortex DW, which remains stable below the Walker field.

IV. DISCUSSION

Firstly, the observed DW propagation behaviour in soft magnetic wires is qualitatively in agreement with previous works [16–18]. Above the Walker field the DW propagation becomes oscillatory with periodical reverse motion, and the Walker period characterizing the spin-structure transformation length, i.e. the displacement distance over the time period between domain wall transformations, becomes smaller with higher applied field. The effect of the periodical wire width modulation can be understood as a result of introducing a spatially oscillating stray field energy that distorts the DW spin structure transformations [24,25,30], resulting in increasing Walker periods (Figure 1). A width modulation with sufficient amplitude and a period smaller than the spin transformation length at a given field is found to suppress the Walker breakdown leading to a steady DW propagation [28,30-32].

However, this simple description is clearly an oversimplification since the simulations here indicate a significant influence of the wire dimensions. For smaller widths and thicknesses, in the case of energetically favourable static

transverse DW states, the periodical wire width modulation greatly affects the propagation and significantly helps to conserve the transverse DW structure. As a result, the Walker breakdown is pushed towards higher fields enabling its full suppression within the FOW. One can find an optimal region of the wire-width modulation period around 50 nm (Figure 3, 100 nm wire width, 10 nm wire thickness and 10% modulation amplitude) corresponding to a fully suppressed Walker breakdown and a gradually reduced effect at higher values (Figure 4).

Larger widths and thicknesses of magnetic wires provide larger nucleation fields and thus a larger FOW [10], which is desirable for most applications. However we observe a significant rise in the depinning field when introducing the periodical wire-width modulation, which is either higher or similar to the rise in the Walker field, thus the wire width modulation does not provide any gain in the DW steady propagation field range.

Undesirable effects of the wire width modulation, i.e. a rise of the depinning field, a reduction of the nucleation field, significanlty reducing the FOW, and a smaller slope of the velocity/applied field curve (Figure 1) with increasing modulation amplitude are observed for all wire geometries. These detrimental effects are minimal for large modulation periods where due to the small edge curvature the DW behaviour resembles an unmodulated wire. Also a significant reduction of the DW propagation fields for wires with smaller widths and thicknesses in the region of low modulation periods in Figure 4b enlarging the FOW is an important finding. The modulation period in this case is close to the DW width, which can be identified as a potential reason for the effect.

The DW propagation through complex structures, including notches, curved shapes, and wire intersections is highly stochastic due to an unpredictable DW spin structure interacting with the edge of the magnetic wire [6,42]. Conserving the DW chirality by suppressing the Walker breakdown significantly reduces or fully eliminates the typical stochastisity of the DW propagation through such complex structures. In particular, the chirality analysis of the DWs propagating through a 90° wire crossing reveals a strong dependence of the behaviour on the exact spin structure: the final propagation direction can in fact be controlled by the DW chirality. Details on an example for DW propagation through an intersection of width-modulated magnetic wires, demonstrating the reduced stochasticity by avoiding chirality-dependent undesired propagation scenarios, can be found in the Supplementary material.

These results clearly show that a definition of the FOW ranging from depinning to nucleation fields is not applicable here: The introduction of additional elements in the design of sensor devices is incompatible with this simple approach described in Ref. [10]: constrictions, expansions, curved regions, and crossings of magnetic wires serve as both anchoring and nucleation centers and can even lead to a narrowing of the actually useful FOW down to zero [11]. The upper limit of the useful FOW of such devices is in fact given by the Walker field and not by the nucleation field. The introduction of a periodic magnetic wire-width modulation narrows the FOW in the definition of Ref. [10], but the obtained suppresion of the Walker breakdown nevertheless enables the reliable operation of such devices within a much larger field range compared to straigt wire edges, so the actually useful FOW in a device is increased. eliminating further elements of the sensor structure or reducing their influence on the FOW. Our approach thus allows to control the naturally occuring stochasticity of the DWs in magnetic wires, which can be also useful for application inneuromorphic computing [7-9].

In conclusion, a comprehensive set of micromagnetic simulations of the influence of wire width modulation on the DW propagation in soft magnetic wires is performed and presented. Key differences in the efficacy of the wire width modulation are observed for wires with different widths and thicknesses such that different domain wall states are energetically stable. In the particular case of magnetic wires with smaller widths and thicknesses, corresponding to the energetically favourable static transverse DWs, periodical wire width modulation with sufficient amplitude and a period smaller than the Walker period at a given field can fully suppress the Walker breakdown and thus makes the DW propagation in magnetic wires and more complex structures fast and reproducible. Our results suggest that periodic width modulation is a promising approach for improving the reliability of DW propagation in devices within an expanded range of the FOW.

SUPPLEMENTARY MATERIALS

The supplementary shows as an example the result of a series of simulations of a field-driven transverse DW passing a wire crossing. Straight DW transmission without altering the state of the side arms is considered a success and everything else a failure. Comparing the result of a crossing of unmodulated wires with one using the modulation showing the optimum FOW above, we find an improved robustness of the DW propagation as a function of field strength and angle, that can be correlated with the preservation of the exact spin structure of the DW in the latter case.

ACKNOWLEDGMENTS

This work has been funded by the European Regional Development Fund (EFRE) and the Federal State of Rhineland-Palatinate under project No 84002616. Additional financial support has been provided by the DFG (SFB TRR 173 Spin+X, Grant No 268565370, projects A01 and B02). This project has received funding from the European Research Council (ERC) under the European Union's Horizon 2020 research and innovation programme under grant agreement 856538.

REFERENCES

[1] Boulle, O.; Malinowski, G.; Kläui, M. Current-Induced Domain Wall Motion in Nanoscale Ferromagnetic Elements. Mater. Sci. Eng. R Rep. 2011, 72 (9), 159–187..

[2] Allwood, D. A.; Xiong, G.; Faulkner, C. C.; Atkinson, D.; Petit, D.; Cowburn, R. P. Magnetic Domain-Wall Logic. Science 2005, 309 (5741), 1688–1692.

[3] Parkin, S. S. P.; Hayashi, M.; Thomas, L. Magnetic Domain-Wall Racetrack Memory. 2008, 320, 190–194.

[4] Diegel, M.; Mattheis, R.; Halder, E. Multiturn Counter Using Movement and Storage of 180 Magnetic Domain Walls. Sens. Lett. 2007, 5 (1), 118–122.

[5] Diegel, M.; Glathe, S.; Mattheis, R.; Scherzinger, M.; Halder, E. A New Four Bit Magnetic Domain Wall Based Multiturn Counter. IEEE Trans. Magn. 2009, 45 (10), 3792–3795.

[6] Borie, B.; Voto, M.; Lopez-Diaz, L.; Grimm, H.; Diegel, M.; Kläui, M.; Mattheis, R. Reliable Propagation of Magnetic Domain Walls in Cross Structures for Advanced Multiturn Sensors. Phys. Rev. Appl. 2017, 8 (4), 044004.

[7] Cui, C., Akinola, O. G., Hassan, N., Bennett, C. H., Marinella, M. J., Friedman, J. S., & Incorvia, J. A. C. Maximized lateral inhibition in paired magnetic domain wall racetracks for neuromorphic computing. Nanotechnology, 2020, 31(29), 294001.

[8] Wang, Y., Yu, H., Ni, L., Huang, G. B., Yan, M., Weng, C., ... & Zhao, J. An energy-efficient nonvolatile in-memory computing architecture for extreme learning machine by domain-wall nanowire devices. IEEE Transactions on Nanotechnology, 2015, 14(6), 998-1012.

[9] Sbiaa, R. Multistate Magnetic Domain Wall Devices for Neuromorphic Computing. physica status solidi (RRL)–Rapid Research Letters, 2021, 15(7), 2100125.

[10] Borie, B.; Kehlberger, A.; Wahrhusen, J.; Grimm, H.; Kläui, M. Geometrical Dependence of Domain-Wall Propagation and Nucleation Fields in Magnetic-Domain-Wall Sensors. Phys. Rev. Appl. 2017, 8 (2), 024017.

[11] Borie, B.; Wahrhusen, J.; Grimm, H.; Kläui, M. Geometrically Enhanced Closed-Loop Multi-Turn Sensor Devices That Enable Reliable Magnetic Domain Wall Motion. Appl. Phys. Lett. 2017, 111 (24), 242402.

[12] Hayward, T. J. Intrinsic Nature of Stochastic Domain Wall Pinning Phenomena in Magnetic Nanowire Devices. Sci. Rep. 2015, 5 (1), 13279.

[13] Hayward, T. J.; Omari, K. A. Beyond the Quasi-Particle: Stochastic Domain Wall Dynamics in Soft Ferromagnetic Nanowires. J. Phys. Appl. Phys. 2017, 50 (8), 084006.

[14] Lage, E.; Mattheis, R.; McCord, J. Stochasticity of Domain Wall Pinning in Curved Ferromagnetic Nanowires Investigated by High-Resolution Kerr Microscopy. J. Magn. Magn. Mater. 2019, 487, 165273.

[15] Kläui, M. Head-to-Head Domain Walls in Magnetic Nanostructures. J. Phys. Condens. Matter 2008, 20 (31), 313001.

[16] Beach, G. S. D.; Nistor, C.; Knutson, C.; Tsoi, M.; Erskine, J. L. Dynamics of Field-Driven Domain-Wall Propagation in Ferromagnetic Nanowires. Nat. Mater. 2005, 4 (10), 741–744.

[17] Mougin, A.; Cormier, M.; Adam, J. P.; Metaxas, P. J.; Ferré, J. Domain Wall Mobility, Stability and Walker Breakdown in Magnetic Nanowires. Europhys. Lett. EPL 2007, 78 (5), 57007.

[18] Schryer, N. L.; Walker, L. R. The Motion of 180° Domain Walls in Uniform Dc Magnetic Fields. J. Appl. Phys. 1974, 45 (12), 5406–5421.

[19] Lee, J.-Y.; Lee, K.-S.; Choi, S.; Guslienko, K. Y.; Kim, S.-K. Dynamic Transformations of the Internal Structure of a Moving Domain Wall in Magnetic Nanostripes. Phys. Rev. B 2007, 76 (18), 184408.

[20] Moore, T. A.; Möhrke, P.; Heyne, L.; Kaldun, A.; Kläui, M.; Backes, D.; Rhensius, J.; Heyderman, L. J.; Thiele, J.-U.; Woltersdorf, G.; Fraile Rodríguez, A.; Nolting, F.; Menteş, T. O.; Niño, M. Á.; Locatelli, A.; Potenza, A.; Marchetto, H.; Cavill, S.; Dhesi, S. S. Magnetic-Field-Induced Domain-Wall Motion in Permalloy Nanowires with Modified Gilbert Damping. Phys. Rev. B 2010, 82 (9), 094445.

[21] Lee, J.-Y.; Lee, K.-S.; Kim, S.-K. Remarkable Enhancement of Domain-Wall Velocity in Magnetic Nanostripes. Appl. Phys. Lett. 2007, 91 (12), 122513.

[22] Brandão, J.; Azzawi, S.; Hindmarch, A. T.; Atkinson, D. Understanding the Role of Damping and Dzyaloshinskii-Moriya Interaction on Dynamic Domain Wall Behaviour in Platinum-Ferromagnet Nanowires. Sci. Rep. 2017, 7 (1), 4569.

[23] Bryan, M. T.; Schrefl, T.; Allwood, D. A. Dependence of Transverse Domain Wall Dynamics on Permalloy Nanowire Dimensions. IEEE Trans. Magn. 2010, 46 (5), 1135–1138.

[24] Weerts, K.; Van Roy, W.; Borghs, G.; Lagae, L. Suppression of Complex Domain Wall Behavior in Ni80Fe20 Nanowires by Oscillating Magnetic Fields. Appl. Phys. Lett. 2010, 96 (6), 062502.

[25] Nakatani, Y.; Thiaville, A.; Miltat, J. Faster Magnetic Walls in Rough Wires. Nat. Mater. 2003, 2 (8), 521–523.

[26] Lewis, E. R.; Petit, D.; O'Brien, L.; Fernandez-Pacheco, A.; Sampaio, J.; Jausovec, A.-V.; Zeng, H. T.; Read, D. E.; Cowburn, R. P. Fast Domain Wall Motion in Magnetic Comb Structures. Nat. Mater. 2010, 9 (12), 980–983.

[27] Ma, X.-P.; Kim, S.-D.; Park, S.-Y.; Choi, Y. S.; Piao, H.-G.; Kim, D.-H. Suppression of Walker Breakdown in Gapped Magnetic Nanowires. J. Appl. Phys. 2018, 124 (8), 083905.

[28] Brandão, J.; Atkinson, D. Controlling the Stability of Both the Structure and Velocity of Domain Walls in Magnetic Nanowires. Appl. Phys. Lett. 2016, 109 (6), 062405.
[29] Piao, H.-G.; Shim, J.-H.; Lee, S.-H.; Djuhana, D.; Oh, S.-K.; Yu, S.-C.; Kim, D.-H. Domain Wall Propagation in Wavy Ferromagnetic Nanowire. IEEE Trans. Magn. 2009, 45 (10), 3926–3929.
[30] Burn, D. M., & Atkinson, D. Suppression of Walker breakdown in magnetic domain wall propagation through structural control of spin wave emission. Applied Physics Letters, 2013, 102(24), 242414.
[31] Burn, D. M.; Arac, E.; Atkinson, D. Magnetization Switching and Domain-Wall Propagation Behavior in Edge-Modulated Ferromagnetic Nanowire Structures. Phys. Rev. B 2013, 88 (10), 104422.
[32] Lee, S.-H.; Shim, J.-H.; Piao, H.-G.; Yu, S.-C.; Oh, S. K.; Kim, D.-H. Micromagnetic Study of Forced Oscillation of Magnetic Domain Wall in Ferromagnetic Nanowires with Variation of Damping Constant. J. Supercond. Nov. Magn. 2012, 25 (8), 2795–2798.
[33] Semenova, E.; Berkov, D.; Gorn, N.; Mattheis, R. Field Operating Window of Nanodevices Employing the Domain Wall Propagation through the Stripes Intersection: Numerical Optimization. J. Appl. Phys. 2018, 124 (15), 153901.
[34] Luo, Z., Hrabec, A., Dao, T.P. et al. Current-driven magnetic domain-wall logic. Nature 2020, 579, 214–218.
[35] Shibata, T., Shinohara, T., Ashida, T., Ohta, M., Ito, K., Yamada, S., Terasaki, Y., and Sasaki, T. Linear and symmetric conductance response of magnetic domain wall type spin-memristor for analog neuromorphic computing. Applied Physics Express 2020, 13 (4), 043004.
[36] OHG, N. M. GMR Multiturn https://www.novotechnik.de/produkte/sensortechnologien/gmr-multiturn/ (accessed 2021 -11 -24).
[37] Vansteenkiste, A.; Leliaert, J.; Dvornik, M.; Helsen, M.; Garcia-Sanchez, F.; Van Waeyenberge, B. The Design and Verification of MuMax3. AIP Adv. 2014, 4 (10), 107133.
[38] Ingvarsson, S., Ritchie, L., Liu, X. Y., Xiao, G., Slonczewski, J. C., Trouilloud, P. L., & Koch, R. H. Role of electron scattering in the magnetization relaxation of thin Ni 81 Fe 19 films. Physical Review B, 66(21), 214416 (2002).
[39] Estévez, V.; Laurson, L. Head-to-Head Domain Wall Structures in Wide Permalloy Strips. Phys. Rev. B 2015, 91 (5), 054407.
[40] Nakatani, Y.; Thiaville, A.; Miltat, J. Head-to-Head Domain Walls in Soft Nano-Strips: A Refined Phase Diagram. J. Magn. Magn. Mater. 2005, 290–291, 750–753.
[41] McMichael, R. D.; Donahue, M. J. Head to Head Domain Wall Structures in Thin Magnetic Strips. IEEE Trans. Magn. 1997, 33 (5), 4167–4169.
[42] Lewis, E. R.; Petit, D.; Thevenard, L.; Jausovec, A. V.; O'Brien, L.; Read, D. E.; Cowburn, R. P. Magnetic Domain Wall Pinning by a Curved Conduit. Appl. Phys. Lett. 2009, 95 (15), 152505.